

A Study on the Characteristics of Two-Phase Flow by Driven Bubbles in a Liquid Bath

Yool-Kwon Oh[†], Dong-Pyo Seo^{*}

Department of Mechanical Engineering, Chosun University, Gwang-ju 375, Korea

^{}Graduate School, Chosun University, Gwang-ju 375, Korea*

Key words: Electro-resistivity probe, Local gas volume fraction, Bubble frequency, Infrared thermo vision camera, PIV (Particle image velocimetry)

ABSTRACT: In the present study, the characteristics of upward bubble flow were experimentally investigated in a liquid bath. An electro-conductivity probe was used to measure local volume fraction and bubble frequency. Since the gas was concentrated at the near the nozzle, the flow parameters were high near the nozzle. In general their axial and radial values tended to decrease with increasing distance. For visualization of flow characteristics, a Particle Image Velocimetry (PIV) and a thermo-vision camera were used in the present study. The experimental results showed that heat transfer from bubble surface to water was largely completed within $z=10$ mm from the nozzle, and then the temperature of bubble surface reached that of water rapidly. Due to the centrifugal force, the flow was more developed near the wall than at bubble-water plume. Vortex flow in the bottom region was relatively weaker than that in the upper region.

Nomenclature

f_B : bubble frequency [s^{-1}]
 N : total number of bubbles
 t : total time [s]
 t_g : time period [s]

Greek symbols

τ_g : gas volume fraction

1. Introduction

There are many industrial processes where gas is injected into a melt or liquid phase in a

bath. These systems are frequently encountered in a metallurgical or in a chemical processing operations. In metallurgical or chemical processes, to inject gas into the liquid bath has some purposes such as mixing, temperature maintenance, and proper of a mechanism for easy process control or a way to add materials for compound metal or chemical reactions. Therefore, in the present study, we carried out the experiments of injecting gas into the liquid bath through the nozzle for the application of gas injection system. For a study on the gas injection system it is very difficult to analyze the flow characteristics because of the complexity of the flow and the irregular motion of bubbles. So many researchers have tried to analyze the flow characteristics by experimental method in the air-water model. In two-phase flow, to improve the design and performance of the device, one has to correctly un-

[†] Corresponding author

Tel.: +82-62-230-7014; fax: +82-62-230-7014

E-mail address: ygoh@mail.chosun.ac.kr

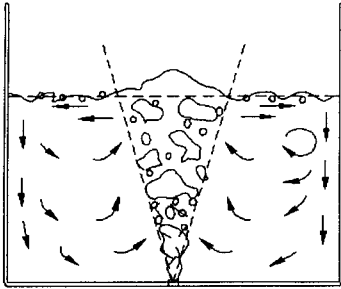


Fig. 1 Schematic diagram for bubble plume and circulation in a bath.

understand the physics of fluid flow.

Figure 1 shows are one of the flow phenomena in the gas injected liquid bath.

Turkoglu⁽¹⁾ measured the local gas volume fraction and bubble frequency using an electro resistivity probe and the temperature of the bubbles and the liquid phase using a micro-thermocouple. According to his research, temperature of the gas phase through the nozzle approached at that of liquid phase in a short time.

Castillejos⁽²⁾ and Castillejos and Brimacombe⁽³⁻⁴⁾ measured the local gas volume fraction and bubble frequency at the each position and the flux using an electro-resistivity probe in the air-water model, after investigating the physical properties of the bubbles in the bubble-liquid plume. They also improved the electro-resistivity probe that was designed to clarify the movement of bubbles by measuring rising velocity of bubbles.

Johansen et al.⁽⁵⁾ and Johansen and Boysan⁽⁶⁾ measured the velocity and turbulence in the liquid in a vertical air injected water bath. A laser doppler system was employed to measure

Table 1 Experimental conditions for the flow measurements

Case	Nozzle dia. [mm]	Vessel dia. [mm]	Bath depth [mm]	Gas flow rate [m ³ /s]
I	1.00	300	200	0.6283×10^{-4}
II	1.00	300	200	1.2566×10^{-4}

the radial and axial mean and fluctuating velocities. Close to the free surface, the mean and turbulent velocities are high and the area of bubble-liquid plume is large.

In the present study, flow parameters such as the local gas volume fraction and bubble frequency were measured using a electro-resistivity probe. Also, the characteristics of two phase flow such as flow shapes, temperature of the bubble and the liquid were investigated using the infrared thermal vision camera and PIV system.

2. Experimental facility and method

The experimental facilities were consisted of the following 4-sections; (1) the test section and the gas delivery system, (2) the data acquisition system and personal computer, (3) the positioning mechanism and the probe, (4) the infrared thermal vision camera and PIV system.

Experimental conditions are given in Table 1. Figure 2 schematically shows the apparatus employed for the measurements.

2.1 Test section and gas delivery system

The test section containing the liquid was built by a transparent acrylic tube and plate.

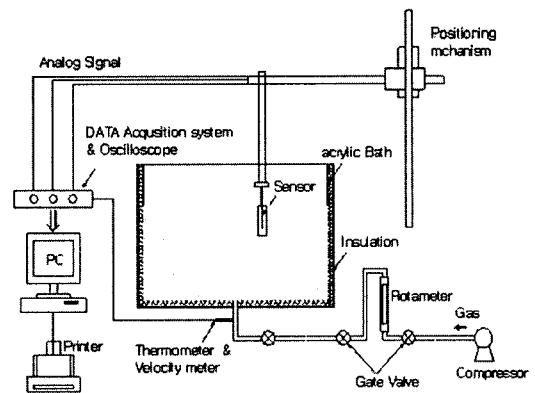


Fig. 2 Schematics diagram of experimental facility.

The bath has inner dimensions of 300 mm×300 mm (diameter×height). Square acrylic box was set-up around the cylindrical bath and water was filled up for visualization and insulation purposes.

Water was filled up to 200 mm in the cylindrical bath. The nozzle which had straight inner hole diameter of 1.0 mm, which was made out of stainless steel and was installed at the bottom center of the bath. The air was supplied by compressor in the laboratory. The air unit keeps the pipe's gauge pressure at 500 kPa and minimizes the flux change by pulsation of air pressure. Gas flow rate was monitored using a rotameter with a spherical float.

2.2 Data acquisition system and personal computer

In order to obtain accurate data through the recursive experiment, positions of the probe should be exactly controlled. Therefore, in the present study, we used a positioning device which could be controlled to 0.1 mm for accurate experiments.

An electro-resistivity probe was used for measurements of the local gas volume fraction and bubble frequency. The shape of the electro-resistivity probe is illustrate in Fig. 3.

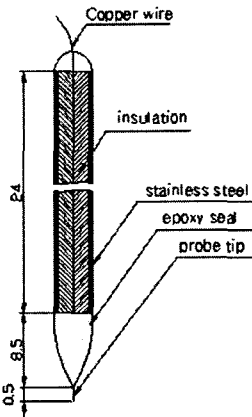


Fig. 3 Schematic diagram of the electro-resistivity probe.

A direct current power supplier was used to capture electrical signal difference between air and water in the bubble-liquid plume. The electrical signals from the probe were displayed on the oscilloscope monitor and were saved using personal computer. The sensing part of the probe composed of a stainless steel needle soldered to a length of copper wire which was straight with the outer diameter of 1.0 mm. The wire passed through an insulating tube which was housed in a stainless steel support tube.

The electrical signals obtained by the probe were stored as waveform in an oscilloscope and as a data file at the personal computer. To measure the temperature of rising bubbles, the infrared thermal vision camera was used.

Anemometer was installed at the bottom of the nozzle to measure the velocity and temperature of injected gas. All the measured data were automatically recorded in a PC.

2.3 Infrared thermal vision camera and PIV system

Every object has its temperature spectrum and emits infrared ray which corresponds to the temperature. When a light is radiated from a body, infrared camera measures temperature distribution by detecting infrared bands among various wavelengths. When many bubbles consecutively arrived at the free surface, we took a shot for imaging the temperature of the bubbles and the liquid phase on the free surface.

The PIV system enables us observe invisible characteristics such as velocity distribution, pressure, kinetic energy, turbulence intensity and

Table 2 Experimental condition of PIV

	Item	Specification
Visualization equipment	Light source	Argon-ion laser
	Sheet light	LLS probe
Measuring condition	Working fluid	Air & water
	Temp.	25°C ± 1
	Particle	Nylon 12

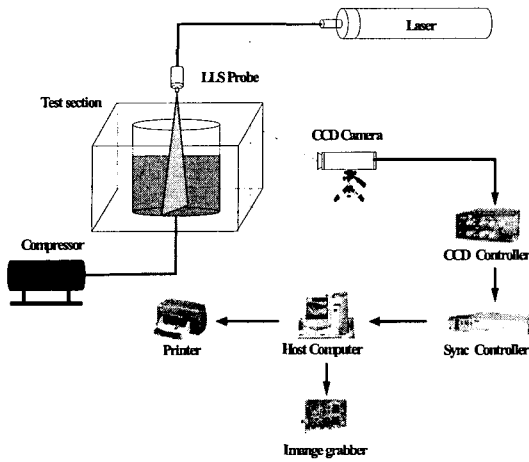


Fig. 4 Schematics diagram of the PIV system.

stress etc.

In the present study, for the visualization of the two-phase flow in a bath, experimental conditions of PIV are shown in Table 2. A typical set-up of a PIV system consists of several sub-systems, including particle seeding, flow field illumination, particle image acquisition, high speed CCD camera and image processing.

A schematic diagram of the PIV system is shown in Fig. 4. Since density of Nylon 12 is almost the same as that of water. Nylon 12 was used as tracer particles. For the illumination of PIV system, an Argon-Ion laser was used, which has the Maximum power output of 7 W. The illumination was provided from the top of the test section to avoid the refraction of light by acrylic resin, as shown in Fig. 4. High speed CCD camera was located perpendicularly with the laser sheet. Frame rate of CCD camera was set up at 30 pps.

3. Results and recommendations

3.1 The local gas volume fraction and bubbles frequency

In order to visualize the movement of bubbles in a bath, the local volume fraction and the bubble frequency were calculated from the

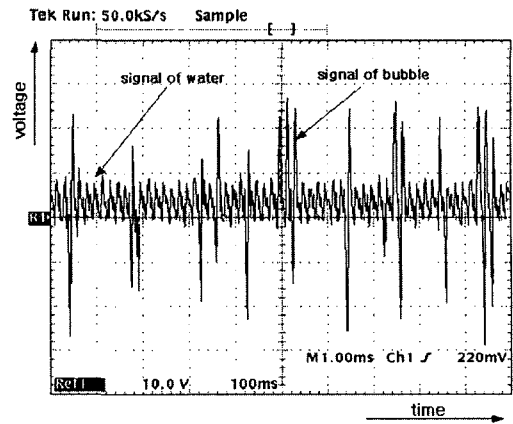


Fig. 5 Electrical signals of bubble captured by an oscilloscope.

electrical signals obtained from the electro-resistivity probe and the oscilloscope.

The experiments were repeatedly 5 times conducted at the same position for 150 second, and the average values were obtained.

Experiments were conducted at 4, 8, 12 and 15 mm in radial direction and from 10 mm to 180 mm in the axis direction (z -axis). Figure 5 shows the electrical signals which were measured at $z=50$ mm from the injection nozzle.

The local gas volume fraction and the bubble frequency were obtained by the following equations;

$$\tau_g = \frac{t_g}{t} \quad (1)$$

$$f_B = \frac{N}{t} \quad (2)$$

where, t is the total sampling time and N is the total number of bubbles detected during the sampling time. The t_g is the time while the bubbles contacted the probe tip.

Figures 6 and 7 show the profiles of bubble frequency and the local gas volume fraction at $z=10$ mm from the injection nozzle with the two different gas flow rate applied. As shown in Figs. 6 and 7, the profiles of the local gas volume fraction and bubbles frequency are sym-

metrical about the axis of the injection nozzle and are bell shapes.

The variation of the local gas volume fraction was about 68% and 82% for Case I and II, respectively. The variation of bubble frequency was about 28 s^{-1} and 44 s^{-1} in Case I

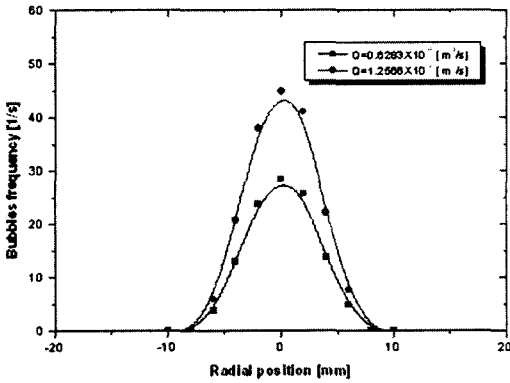


Fig. 6 Bubbles frequency at $z=10\text{ mm}$.

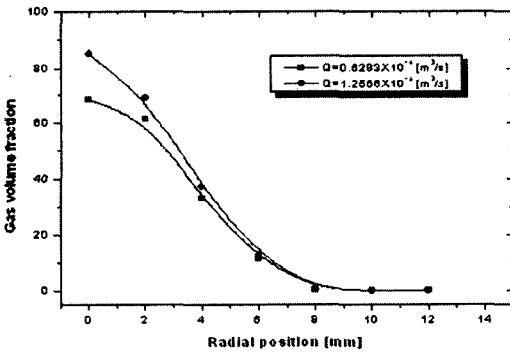


Fig. 7 Gas volume fraction at $z=10\text{ mm}$.

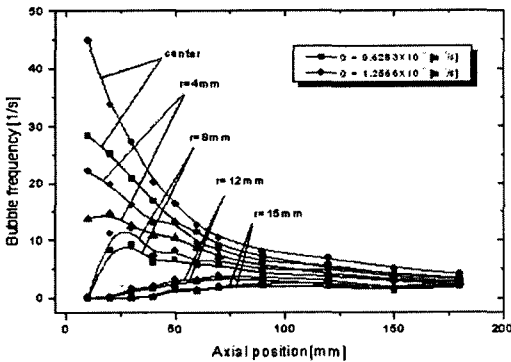


Fig. 8 Axial profiles of the bubble frequency.

and II, respectively. These results reveal that the more the gas flow rate increase, the more the variations of gas volume fraction and bubble frequency increase.

Figure 8 shows the profiles of the bubble frequency in the axial and the radial direction. As shown in Fig. 8, as the gas flow increases the bubble frequency increases, but the variations of the bubble frequency are almost similar above $z=60\text{ mm}$ from the axis of injection nozzle.

3.2 Analysis of temperature and flow structure

Temperature measurements of bubbles and liquid were carried out in using an infrared thermal vision camera. The measurements were performed at different points along the axis of the injection nozzle. Initial temperatures of air and water were 22°C and 60°C , respectively. Figure 9 shows image and temperature distributions of the bubble and the liquid phase on the free surface at $z=50\text{ mm}$. The spots in the pictures indicate bubbles and the shape when appeared on the surface.

Infrared thermal vision camera was situated at 1 m from the subject and its emissivity was 0.85.

Figure 10 shows the temperature distribution of bubbles at several positions (i.e., $z=5\text{ mm}$, 10 mm , and 50 mm) from the gas injection nozzle. As shown in Fig. 10, the temperature of bubble is about 45°C at $z=5\text{ mm}$ and about

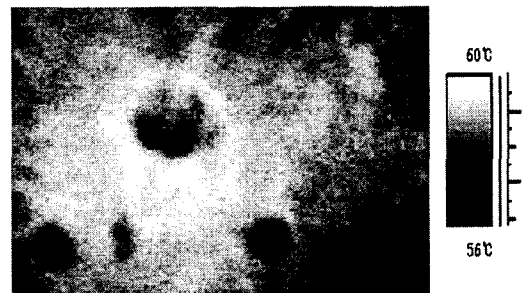


Fig. 9 Temperature of bubble at $z=50\text{ mm}$.

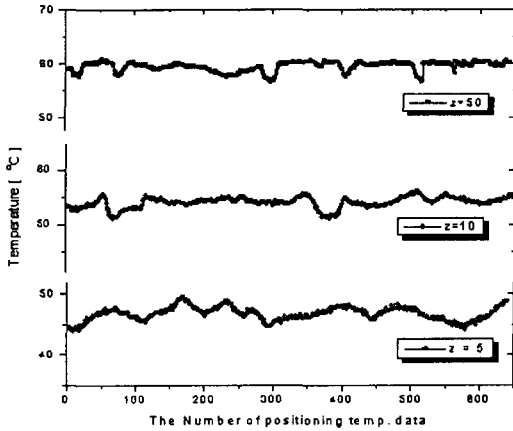


Fig. 10 Distribution of bubbles temperature at different axial position.

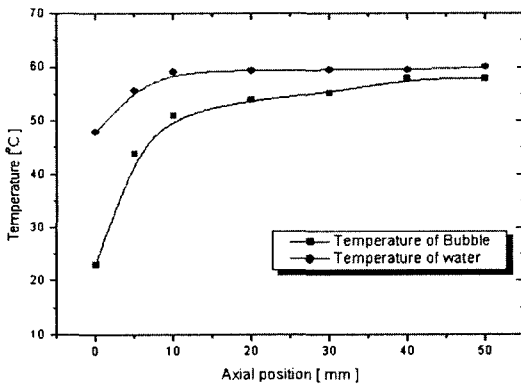


Fig. 11 Liquid and gas temperature profiles along the axis of the injection nozzle.

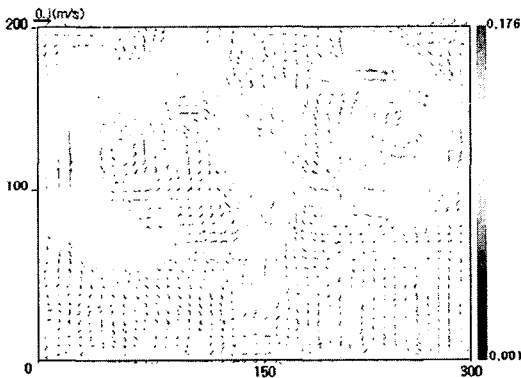


Fig. 12 Velocity vectors in the flow field using PIV system.

53°C at $z=10$ mm.

Figure 11 displays the temperature variation of bubbles and water along the axis of injection nozzle. As shown in Fig.11, the temperature of bubbles changed rapidly within the $z=10$ mm, and after that the temperature of bubble changed slowly.

As a result, heat transfer from the water to the bubble was almost achieved within $z=10$ mm from the nozzle and after that the temperature of bubble surface became similar to liquid phase.

The characteristics of liquid circulation flow were visually studied using PIV system for $0.62 \text{ m}^3/\text{s}$ gas flow rate. Velocity vectors in the flow field were obtained through the image processing procedure. Typical velocity vector of flow in the bath were presented in Fig. 12. As shown in Fig.12 developed flows in both wall sides and upper region were observed.

When gas is injected in the liquid bath, kinetic energy is concentrated in the center. Because bubbles rise on the free surface, centrifugal force occurs in the liquid region. The more the gas flow rate increases, the stronger the centrifugal force is. Finally, because the velocity profiles in the both side wall are increasing by the centrifugal force, the fluid flow is developed near the free surface and both side wall.⁽⁷⁾ As shown in Fig.12, the flow in the lower region of bath is considerably weak. It is known as the dead zone.

4. Conclusions

(1) When the gas flow rate is increased, the profiles of the local gas volume fraction and bubble frequency are increased. However, they were almost similar above $z=60$ mm.

(2) The heat transfer phenomenon from bubble surface to liquid phase was almost achieved within $z=10$ mm from the nozzle after that, the temperature of bubble surface became similar

to liquid phase in a short time.

(3) Due to upward motion of bubbles and centrifugal force, the fluid flow was developed near the free surface and both side wall. Dead zone existed in the lower region.

References

1. Turkoglu, H., 1990, Transport processes in gas-injected liquid baths, Ph.D. Thesis, Drexel University, Philadelphia.
2. Castillejos, A., 1986, A study of the fluid-dynamic characteristics of turbulent gas-liquid bubble plumes, Ph.D. Thesis, The University of British Columbia, Canada.
3. Castillejos, A. H. and Brimacombe, J. K., 1986a, Measurement of physical characteristics of bubbles in gas-liquid plumes, Part I: An improved electro-resistivity probe technique, Metallurgical Transactions B, Vol. 18B, pp. 649-658.
4. Castillejos, A. H. and Brimacombe, J. K., 1986b, Measurement of physical characteristics of bubbles in gas-liquid plumes, Part II: Local properties of turbulent air-water plumes in vertically injected jets, Metallurgical Transactions B, Vol. 18B, pp. 659-671.
5. Johansen, S. T., Robertson, D. G. C., Woje, K. and Engh, T. A., 1988, Fluid dynamics in bubble stirred ladles, Part I: Experiments, Metallurgical Transactions B, Vol. 19B, pp. 745-754.
6. Johansen, S. T. and Boysan, F., 1988, Fluid dynamics in bubble stirred ladles, Part II: Mathematical modeling, Metallurgical Transactions B, Vol. 19B, pp. 755-764.
7. Sohn, H. C., 2000, A study on the flow characteristics of developing turbulent steady, turbulent oscillatory and turbulent pulsating flows in the entrance region of a curved duct, Ph.D. Thesis, Chosun University, Korea.